Carbohydrate Polymers 110 (2014) 329–337

Contents lists available at ScienceDirect

Carbohydrate Polymers

journal homepage: www.elsevier.com/locate/carbpol

Development of a myricetin/hydroxypropyl-β-cyclodextrin inclusion complex: Preparation, characterization, and evaluation

Yashu Yao[a,b], Yan Xie[b,*], Chao Hong[b], Guowen Li[c,**], Hongyi Shen[b], Guang Ji[a]

[a] Institute of Chinese Materia Medica, Shanghai University of Traditional Chinese Medicine, Shanghai, China
[b] Research Center for Health and Nutrition, Shanghai University of Traditional Chinese Medicine, Shanghai, China
[c] Pharmacy Department, Shanghai TCM-Integrated Hospital, Shanghai, China

ARTICLE INFO

Article history:
Received 12 February 2014
Received in revised form 19 March 2014
Accepted 6 April 2014
Available online 18 April 2014

Keywords:
Myricetin
Hydroxypropyl-β-cyclodextrin
Inclusion complex
Characterization
In vitro dissolution
Pharmacokinetics

ABSTRACT

Myricetin shows low oral bioavailability (<10%) in rats due to poor aqueous solubility, though it has various pharmacological activities. Complexation with cyclodextrins (CDs) is a potent pharmaceutical method to enhance the bioavailability of poorly soluble compounds. The myricetin/HP-β-CD inclusion complex was prepared and confirmed by DSC, PXRD, and SEM. Here, the inclusion mode is described in detail with regard to structural and energetic aspects using a phase solubility diagram and ^{1}H NMR, NOESY, and FT-IR spectra. The water solubility and dissolution rate of myricetin were greatly enhanced by forming the myricetin/HP-β-CD inclusion complex. Consequently, the oral bioavailability of the myricetin/HP-β-CD inclusion complex in rats was effectively increased 9.4-fold over free myricetin, and its antioxidant activity was also improved. The present study provides useful information for the potential application of complexation with myricetin, a naturally occurring hydrophobic phenolic compound in herbal medicine.

1. Introduction

Myricetin (3,5,7,3′,4′,5′-hexahydroxyflavone) is a naturally occurring flavonoid commonly found in tea, berries, fruits, vegetables, and medicinal herbs (Li & Ding, 2012). As a bioactive component, myricetin has been reported to exhibit various effects, such as anti-oxidative (Ong & Khoo, 1997), anti-carcinogenic (Phillips, Sangwan, Borja-Cacho, Dudeja, Vickers, & Saluja, 2011), prevention of platelet aggregation (Liu, Tzeng, Liou, & Lan, 2007), and cytoprotective (Dajas et al., 2003) effects. As a result, myricetin has a variety of therapeutic applications, including as a cardiovascular protective agent (Li & Ding, 2012), a hepatoprotective agent (Maheshwari, Yogendra Kumar, Verma, Singh, & Singh, 2011), and potentially the treatment of colorectal carcinoma (Ko, Shen, Lee, & Chen, 2005). However, myricetin has been shown to be essentially insoluble (16.60 μg/mL) (Yao et al., 2014), which typically results in poor and erratic oral absorption. As expected, the C_{max} of myricetin was only 10.38 ± 1.87 ng/mL after oral administration of an equivalent dose of myricetin 3.95 mg/kg extracted from Abelmoschi Corolla (Lu et al., 2013), and the absolute bioavailability in rats was only 9.62% according to our previous research (Dang et al., 2013), confirming that the oral absorption of myricetin is very limited. It is well known that the therapeutic effects of active pharmaceutical ingredients (APIs) are closely related to their oral bioavailability. Therefore, it follows that the clinical application of myricetin would be hindered by its pharmacodynamic properties. Valid strategies such as pharmaceutical approaches or delivery systems to promote the solubility, absorption, and therapeutic potential of myricetin are of the utmost importance.

To date, many formulation approaches, such as salt formation (Burton et al., 2012), particle size reduction (e.g., nanosuspensions or drug nanocrystals) (Sigfridsson, Lundqvist, & Strimfors, 2009; Sahoo et al., 2011; Han, Yu, Guo, Wang, Kuang, & Wang, 2014), amorphous solid dispersions (Adibkia et al., 2013), prodrugs (Kim, Park, et al., 2009), and complexation (e.g., cyclodextrins) (Reddy, Rehana, Ramakrishna, Chowdhary, & Diwan, 2004; Jullian, Moyano, Yañez, & Olea-Azar, 2007), have been employed to improve the solubility of compounds in the gastrointestinal tract and, consequently, improve their oral bioavailability. Of these techniques, complexation with cyclodextrins (CDs) is comparatively traditional and straightforward, as it allows poorly soluble compounds to

* Corresponding author at: Research Center for Health and Nutrition, Shanghai University of Traditional Chinese Medicine, 1200 Cailun Road, Shanghai 201203, China. Tel.: +86 21 51322440; fax: +86 21 51322407.
** Corresponding author at: Pharmacy Department, Shanghai TCM-Integrated Hospital, 184 Baoding Road, Shanghai 200082, China. Tel.: +86 21 65556806; fax: +86 21 65556806.
E-mail addresses: rosexie_1996@hotmail.com (Y. Xie), lgwshutcm@163.com (G. Li).

http://dx.doi.org/10.1016/j.carbpol.2014.04.006
0144-8617/

spontaneously enter the nonpolar cavity of CDs and enhance their hydrophilicity while retaining the original chemical composition. CDs are cyclic oligosaccharides derived from starch containing six (α-CD), seven (β-CD), eight (γ-CD), or more (α-1,4)-linked α-D-glucopyranose units. At present, β-CD is the most commonly employed CD in pharmaceutical products compared to the other natural CDs due to its favorable cavity size for encapsulation of drug molecules, easy production, and relatively economic price.

However, β-CD exhibits some disadvantages, such as its limited aqueous solubility, the potential formation of crystalline complexes, and nephrotoxicity when administered parenterally (Stegemann, Leveiller, Franchi, de Jong, & Linden, 2007). To address the unfavorable characteristics of β-CD, many β-CD derivatives have been prepared through various chemical modifications. HP-β-CD is a hydroxyalkylated β-CD derivative that exhibits relatively high water solubility, low toxicity, and satisfactory inclusion ability (Gould & Scott, 2005). With these advantages, HP-β-CD has been successfully used to improve the pharmaceutical properties of APIs and exhibits a better potential for application than β-CD. Additionally, HP-β-CD has been reported to possess higher stability constant ($390.6\ M^{-1}$) than β-CD ($250.3\ M^{-1}$) with rutin (Nguyen, Liu, Zhao, Thomas, & Hook, 2013), implying a better spatial relationship and complexing capability with rutin. The irbesartan/HP-β-CD complex also has a significantly enhanced dissolution rate from tablets (Kane, Naik, Bumrela, & Kuchekar, 2009) compared to that of the irbesartan/β-CD complex.

Given the increased solubility, enhanced dissolution, and stabilizing effect, HP-β-CD could also be applied to encapsulate effective components in herbal medicine. It has been proven to significantly increase the solubility (approx. 15-fold) of alpinetin (Ma et al., 2012) and the oral bioavailability (approx. 3-fold) of rutin (Miyake et al., 2000), which will be beneficial to the therapeutic application of these two compounds. Moreover, the hydrolytic stability of curcumin under neutral–alkaline conditions has been improved by complexing with HP-β-CD (Ouyang et al., 2011). Obviously, HP-β-CD has a significant potential to enhance the solubility, stability, and bioavailability of active components separated from herbs.

Therefore, the present work focused on encapsulating myricetin within an HP-β-CD complex, aiming to form a simple, stable, and effective formulation. The characterizations were investigated comprehensively, and the complex properties were elucidated by phase-solubility diagrams, nuclear magnetic resonance (^{1}H-NMR) spectroscopy, and two-dimensional rotational frame nuclear Overhauser effect spectroscopy (2D NOESY). The in vitro and in vivo properties of myricetin as a myricetin/HP-β-CD inclusion complex, including solubility, dissolution rate, radical scavenging ability, and oral bioavailability, were also evaluated.

2. Materials and methods

2.1. Materials

Myricetin with purity greater than 98% (standard substance in HPLC analysis) was obtained from Shanghai Tauto Biotech Co., Ltd. (Shanghai, China). The raw material myricetin (yellow powder, purity ≥90%) was purchased from Shanghai DND Pharm-Technology Co., Inc. (Shanghai, China). HP-β-CD was purchased from Shanghai yuanye Bio-Technology Co., Ltd (Shanghai, China). 2, 2-diphenyl-1-picrylhydrazyl (DPPH) was purchased from Aladdin, Inc., St (Shanghai, China). β-glucuronidase and sulfatase were purchased from Sigma–Aldrich (St. Louis, MO, USA). HPLC grade acetonitrile and methanol were purchased from Honeywell Burdick & Jackson (Ulsan, Korea); formic acid was obtained from Fluka (Burchs, Switzerland). Ultra-pure deionized water was generated from a Millipore Milli-Q Gradient System (Billerica, MA, USA). Ascorbic acid, carboxymethylcellulose sodium (CMC-Na), anhydrous ethanol, Tween-80, and other chemicals were of analytical grade and purchased from Sinopharm Chemical Reagent Co., Ltd. (Shanghai, China).

2.2. Preparation of myricetin/HP-β-CD inclusion complex

Inclusion complex of myricetin and HP-β-CD was prepared by the suspension method (Ma et al., 2012). In a typical procedure, myricetin was dissolved in anhydrous ethanol and then added to an aqueous solution of an appropriate amount of HP-β-CD. The resulting mixture was kept in a thermostatic water bath (40 °C) and shaken for 24 h to reach equilibrium. After filtering to remove the undissolved raw material, the residue was dried in a rotary evaporator and the solid products were collected. The dried mass was further pulverized and then dried under high vacuum.

A physical mixture (PM) was also prepared by simply mixing myricetin and HP-β-CD at the same ratio as for inclusion in a mortar and pestle for 5 min to obtain a homogeneous blend.

2.3. Characterization of myricetin/HP-β-CD inclusion complex

2.3.1. Differential scanning calorimetry (DSC)

The crystallinity of myricetin and its complex was characterized by DSC on a Differential Scanning Calorimeter DSC 822e (Mettler Toledo, Greifensee, Switzerland) calibrated for temperature and cell constants using indium. Samples were placed on non-hermetic aluminum pans. The sample cell was equilibrated at 25 °C and then heated at a rate of 10 °C/min in a range of 50–400 °C.

2.3.2. Fourier-transform infrared spectroscopy (FT-IR)

FT-IR spectra were recorded using a Nicolet FT-IR-R330 spectrophotometer (ThermoFisher Scientific, MA, USA). The samples of myricetin, HP-β-CD, their physical mixture, and their complex were previously ground and mixed thoroughly with KBr. The KBr disks were prepared by compressing the powder and the spectra were recorded in the scanning range was 400–4000 cm^{-1}.

2.3.3. Powder X-ray diffractometry (PXRD)

The PXRD patterns of myricetin, HP-β-CD, their physical mixture, and their inclusion complex were obtained at ambient temperature using a Shimadzu XRD-6000X X-ray diffractometer (Shimadzu, Kyoto, Japan). The samples were irradiated with a Ni-filtered Cu-K (α) radiation, at a voltage of 40.0 kV and a current of 40.0 mA. The scanning rate was employed for 2°/min over a diffraction angle of 2θ ranging from 3° to 50°.

2.3.4. Scanning electron microscopy (SEM)

Morphological evaluation of myricetin, HP-β-CD, the myricetin/HP-β-CD inclusion complex, and a physical mixture of myricetin and HP-β-CD was performed by SEM (Philips XL-30, Eindhoven, Holland). A small piece of the double-sided adhesive tape was fixed onto an aluminum stub, and the powders were sprinkled and dispersed on the stub surface. Prior to examination, the samples were sputter coated with gold–palladium under argon atmosphere to render them electrically conductive.

2.3.5. Nuclear magnetic resonance spectroscopy (NMR)

NMR experiments were performed at 298 K on an Advance III 600 MHz spectrometer equipped with a 5 mm PABBO probe (Bruker Corporation, Fällanden, Switzerland). ^{1}H-NMR spectra of myricetin, HP-β-CD and the myricetin/HP-β-CD inclusion complex were obtained by individually dissolving them in 0.5 mL of DMSO-d_6 or D_2O. 2D NOESY was performed using the standard Bruker pulse program Noesygpph, and the samples were dissolved in DMSO-d_6. For NOESY spectra, the time domain data was zero

filled to 1024 points in F2 and 466 points in F1. The NOESY data was acquired with a mixing time of 0.7 s, and a relaxation delay of 2 s. All data were acquired and processed using Bruker's Topspin 3.0 software.

2.4. In vitro evaluations

2.4.1. Phase solubility studies

Phase solubility studies were carried out in water according to the method previously reported by Higuchi and Connors (1965). Briefly, excess amounts of myricetin were added to 10 mL of aqueous solution containing various concentrations of HP-β-CD (0–10 mM). The suspensions were vigorously shaken with a shaking rate of 120 rpm in water bath for 36 h at 25 °C and 37 °C, respectively. After attaining equilibrium, the samples were centrifuged (13,000 rpm, 10 min), and then the concentration of myricetin in supernatant liquid was analyzed by HPLC (Yao et al., 2014). The apparent stability constants (K_s) were calculated from the phase solubility diagrams, according to the following Eq. (1) (Ge, Huang, Tian, Huang, & Zeng, 2012), where S_0 is the solubility of myricetin in the absence of HP-β-CD.

$$K_s = \frac{\text{Slope}}{S_0(1\text{-Slope})} \tag{1}$$

Other thermodynamic parameters can be obtained as a function of the temperature and stability constant. The change in Gibbs' free energy (ΔG) in the complexing process was determined using Eq. (2), where R is the universal gas constant (8.314 J mol^{-1} K^{-1}) and T is temperature in Kelvin (Jun et al., 2007).

$$\Delta G_i = -RT_i \ln K_i \tag{2}$$

Furthermore, the enthalpy change (ΔH) for the HP-β-CD/myricetin binary system was investigated using the Van't Hoff equation as shown below (Eq. (3)) where K is as defined above, and ΔS (Eq. (4)) is the entropy change (Jun et al., 2007).

$$\ln \frac{K_2}{K_1} = \frac{\Delta H}{R} \times \frac{T_2 - T_1}{T_2 T_1} \tag{3}$$

$$\Delta S_i = \frac{\Delta H_i - \Delta G_i}{T_i} \tag{4}$$

2.4.2. Dissolution studies

The in vitro dissolution studies of the pure drug, physical mixture, and complex were conducted in a dissolution apparatus RCZ-6C1 (Huanghai Medicine & Drug Testing Instruments, Shanghai, China) using the paddle method according to USP35-NF30. In the present studies, samples equivalent to 25 mg of myricetin were taken into the dissolution vessel containing 900 mL dissolution medium (0.1% Tween-80). The paddle was rotated at 50 rpm, and the temperature of the dissolution medium was maintained at 37 ± 0.5 °C. The samples (10 mL) were withdrawn at predetermined time intervals (1, 5, 10, 20, 40, 60, 120, 240 min) and replaced with the same volume of fresh medium. All samples were filtered through a 0.45 μm membrane filter and analyzed by HPLC, as described above. All tests were performed in triplicate.

2.4.3. Assay of antioxidant activities

The antioxidant activity of the myricetin/HP-β-CD inclusion complex was compared to myricetin by DPPH radical scavenging assay (Villaño, Fernández-Pachón, Moyá, Troncoso, & García-Parrilla, 2007; Lucas-Abellán, Mercader-Ros, Zafrilla, Gabaldón, & Núñez-Delicado, 2011). Briefly, a 0.1 mM solution of DPPH in ethanol was prepared. A series of concentrations of pure myricetin and its complex were dissolved in appropriate solvents and diluted. Then, 2 mL of DPPH was added to 2 mL of sample solutions at different concentrations, and the mixture was incubated at room temperature for 30 min. The absorbance was measured at 517 nm using a UV754 N UV–vis spectrophotometer (Lengguang Tech., Shanghai, China). Lower absorbance of the reaction mixture indicated higher free radical scavenging activity. The DPPH scavenging effect (K) was calculated using Eq. (5) (Yuan, Du, Jin, & Xu, 2013): where $A_{control}$ was the absorbance of the blank control of the DPPH solution, A_{sample} was the absorbance of the DPPH solution after incubation with the samples, and A_{blank} was the absorbance of the samples alone. The experiment was performed in triplicate.

$$K = \frac{A_{control} - (A_{sample} - A_{blank})}{A_{control}} \times 100\%. \tag{5}$$

2.5. In vivo pharmacokinetics

2.5.1. Animals and treatment

Healthy male Sprague-Dawley rats (280–300 g) were supplied by the Laboratory Animal Center, Shanghai University of Traditional Chinese Medicine, China. Prior to the experiments, the rats were housed in a temperature and humidity controlled room (20–25 °C, 55 ± 5% air humidity) with 12 h light/dark cycles and free access to water and standard rat chow. All animal experiments were carried out in accordance with the local institutional guidelines for animal care of Shanghai University of Traditional Chinese Medicine.

2.5.2. Pharmacokinetic studies

The rats were fasted overnight with free access to water prior to experiments. Twelve rats were randomly divided into two groups (six rats in each group), and given either myricetin or the prepared complex at a dose of 50 mg/kg or 25 mg/kg of myricetin, respectively. Myricetin or its complex powders were dispersed homogeneously in 0.5% CMC-Na (Zhang, Huang, Liu, Gao, & Qian, 2013) aqueous solution to form suspensions before gavage administration to rats. Blood samples were collected from the oculi chorioideae vein into a heparinized tube at predetermined time points (0, 0.25, 0.5, 1, 2, 4, 6, 8, 10, 12, 16, 24, and 48 h). After centrifugation at 13,000 rpm for 10 min, the plasma layer (100 μL) was immediately transferred to clean tubes and stored at −80 °C until analysis. Plasma preparation and myricetin quantification were performed as described by Dang et al. (2013).

2.5.3. Pharmacokinetic data analysis

Pharmacokinetic parameters were estimated by non-compartmental modeling using DAS 2.1.1 (Mathematical Pharmacology Professional Committee of China, Shanghai, China). The results were expressed as the mean ± standard deviation (SD). Student's t-test was performed to compare groups and $p < 0.05$ was considered significant.

The relative bioavailability after oral administration was calculated in Eq. (6):

$$F(\%) = \frac{\text{AUC}_{complex}}{\text{AUC}_{myricetin}} \times \frac{\text{dose}_{myricetin}}{\text{dose}_{complex}} \tag{6}$$

F represents the relative bioavailability, and AUC represents the area under the curve.

3. Results and discussion

3.1. Characterization of myricetin inclusion complex

3.1.1. DSC analysis

The DSC thermograms of myricetin, HP-β-CD, the physical mixture, and the prepared complex are shown in Fig. 1A. There is an endothermic peak at 355 °C in the DSC thermogram of pure myricetin, corresponding to its melting point recorded in SciFinder. However, in the thermal profile of HP-β-CD physical mixture,

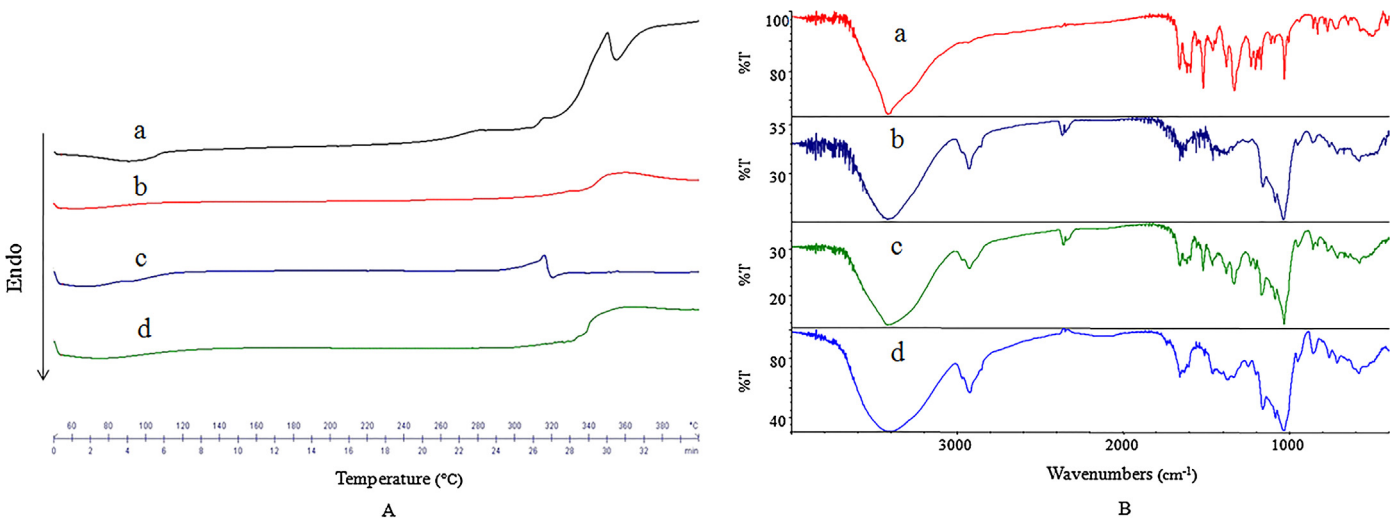

Fig. 1. DSC thermograms (A) and FT-IR spectra (B) for the raw myricetin (a), HP-β-CD (b), physical mixture (c), and myricetin/HP-β-CD inclusion complex (d).

the characteristic peak was slightly shifted to lower temperature, roughly 320 °C, which demonstrates that there is a weak interaction between myricetin and HP-β-CD (de Freitas et al., 2012). Comparatively, HP-β-CD and the inclusion complex gave an almost smooth DSC curve in the investigated temperature interval with no thermal signal, indicating the amorphous characteristic of these two samples. Additionally, the thermogram of the physical mixture was similar to the superimposition of the thermograms of individual myricetin and HP-β-CD, indicating that a true complex has not formed in the physical mixture. In contrast, the endothermic peak of myricetin was completely absent in the thermal profile of the complex, which suggested that the drug was incorporated into the cavity of HP-β-CD and subsequently formed the amorphous complex (Pandit, Gorantla, Devi, Pai, & Sarasija, 2011).

3.1.2. FT-IR analysis

The FT-IR spectra of myricetin, HP-β-CD, their physical mixture, and inclusion complex are shown in Fig. 1B. For myricetin, the band at 3415 cm^{-1} is assigned to a free —OH bond vibration; 1663 cm^{-1} and 1618 cm^{-1} are assigned to the stretching vibration of the C=O group that appears as a very strong doublet; 1554 cm^{-1} is denoted for the stretching vibration of C=C in the hexatomic ring; 1520 cm^{-1} is assigned to an aromatic group; and 1326 cm^{-1} and 1168 cm^{-1} are assigned to the C—O—C vibration, which was similar to quercetin (Kakran, Sahoo, & Li, 2011). The spectrum of HP-β-CD can be characterized by the intense band at 3407 cm^{-1}, corresponding to vibration of the hydrogen-bonded OH groups, the band at 2926 cm^{-1} assigned to absorption by the CH and CH_2 groups, and some other prominent peaks at 1654 cm^{-1} (H—O—H bending), 1156 cm^{-1} (C—O), and 1032 cm^{-1} (C—O—C). In the spectra of physical mixtures, all characteristic bonds of myricetin and HP-β-CD were evident, indicating weaker or no interaction between myricetin and HP-β-CD when physically mixed. However, in the spectra of myricetin/HP-β-CD inclusion complex, some characteristic bands of myricetin were shifted or absent. For example, the absorption bands of C=O (at 1663 cm^{-1} and 1618 cm^{-1}) and C—O—C (at 1326 cm^{-1} and 1168 cm^{-1}) vibration were not observed, indicating that the vibration of these two group on C rings may have been restricted due to the formation of the inclusion complex. In addition, C=C (1554 cm^{-1}) was not observed, and signals from aromatic groups (1520 cm^{-1}) were slightly shifted to 1511 cm^{-1} and greatly weakened, indicating that either a majority of hexatomic rings of myricetin were included within HP-β-CD or only one of the two hexatomic rings in some myricetin molecules was included.

3.1.3. PXRD analysis

The crystalline states of myricetin, HP-β-CD, their physical mixture, and inclusion complex were examined by powder X-ray diffraction and illustrated in Fig. 2A. As indicated in the diagram, myricetin displayed a series of intense peaks, indicating its crystalline form, whereas HP-β-CD showed an amorphous state that lacked crystalline peaks. The PXRD pattern of the physical mixture exhibited the feature of amorphous cyclodextrins, whereas some crystalline peaks of myricetin were clearly distinguished. Therefore, the pattern of the physical mixture was possibly the superimposition of the patterns of myricetin and HP-β-CD, suggesting there no new crystals formed. However, the inclusion complex noted an amorphous halo pattern from the diffractogram, in which the sharp diffraction peaks of myricetin completely disappeared. These results further proved that myricetin had been incorporated into the cavity of HP-β-CD and presented as the amorphous or disordered structure.

3.1.4. SEM analysis

SEM photographs of myricetin, HP-β-CD, their physical mixture and inclusion complex are shown in Fig. 2B. Myricetin shows a needle-like crystal, and the typical structure of HP-β-CD appeared as amorphous, spherical particles with cavity structures. The physical mixture of myricetin/HP-β-CD reveals some similarities with the crystal of the two free molecules and shows both crystalline and amorphous components exist. However, for the inclusion complex, the original morphology of myricetin had completely disappeared, and it was impossible to differentiate the two components of myricetin and HP-β-CD. This drastic change in particle shape and morphology in Fig. 2B (d) was indicative of the presence of an apparent interaction between myricetin and HP-β-CD, most likely due to the formation of the inclusion complex (Delrivo, Zoppi, & Longhi, 2012).

In addition, the inclusion complex appeared as homogeneous and amorphous in the SEM graph, which agrees with the DSC and PXRD results mentioned above. All results indicate the formation of an inclusion complex between myricetin and HP-β-CD and demonstrate that no complex is formed by their physical mixture. However, the molecular mechanism of complex formation is still unclear and needs to be further elucidated.

3.1.5. NMR analysis

^1H NMR spectrum provides the most direct and powerful evidence for the formation of the inclusion complex. If a guest

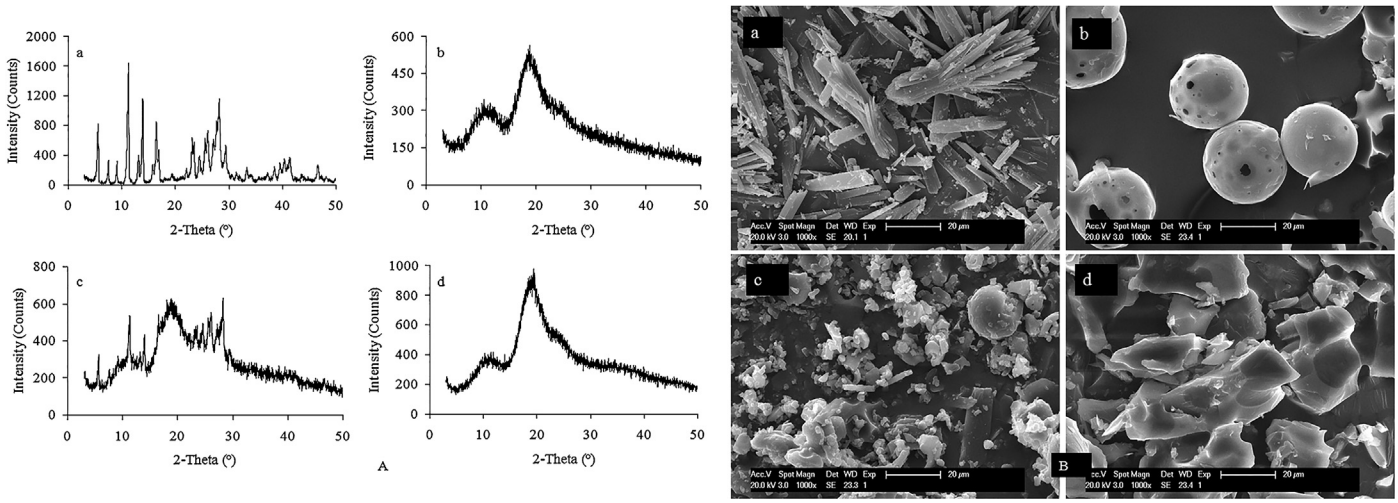

Fig. 2. Powder X-ray diffractogram (A) and Scanning electron microphotographs (B) for the raw myricetin (a), HP-β-CD (b), physical mixture (c), and myricetin/HP-β-CD inclusion complex (d).

molecule is incorporated into the HP-β-CD cavity, the screening constants of the HP-β-CD protons inside the cavity (H-3 and H-5) should be sensitive to the changed environment, but that of the outside protons (H-1, H-2, and H-4) should not. This would result in chemical shift changes of the protons incorporated within the complex (Yuan, Jin, & Xu, 2012). To explore the possible inclusion mode of the myricetin/HP-β-CD complex, we compared the ^{1}H-NMR spectrums of myricetin, HP-β-CD, and the inclusion complex in DMSO-d_6 (Fig. 3A). The majority of myricetin protons displayed chemical shifts at δ 6.0–12.5 ppm, which were distinct from the HP-β-CD protons (δ 1.0–5.5 ppm). In the low-field region, two doublet aromatic proton signals at δ 6.19 (1H, d, J = 1.9 Hz, H-6) and 6.38 (1H, d, J = 1.9 Hz, H-8), a singlet aromatic proton signal at δ 7.25 (2H, brs, H-2′ and H-6′), and six phenolic hydroxyl signals at δ 8.82 (1H, s, OH-4′), 9.23 (2H, OH-3′ and OH-5′), 9.35 (1H, s, H-3), 10.79 (1H, s, OH-7), and 12.51 (1H, s, OH-5) were clearly observed. However, all $\Delta\delta$ (variations of the chemical shifts) values are $\leq$0.01 ppm (data not shown), which indicated the myricetin/HP-β-CD inclusion complex had a negligible difference to both myricetin and HP-β-CD.

Two-dimensional (2D) NMR spectra provide some important information about the spatial proximity between host and guest atoms by observation of intermolecular dipolar cross-correlations. Because $\Delta\delta$ values were negligible in the ^{1}H NMR experiment, 2D NOESY data of myricetin/HP-β-CD inclusion complex were obtained (dissolved DMSO-d_6) to gain more conformational information. All expected aromatic proton signals for the complex were clearly observed in the acquired ^{1}H-NMR spectrum (Fig. 3A): δ 6.19 (1H, d, J = 1.9 Hz, H-6), 6.38 (1H, d, J = 1.9 Hz, H-8), and δ 7.25 (2H, brs, H-2′, and H-6′). Because myricetin is essentially insoluble in water, the spectrum presented direct evidence for the inclusion of myricetin inside the CD cavity. As expected, the NOESY spectrum of myricetin/HP-β-CD complex in DMSO-d_6 (Fig. 3B) showed key correlations of OH-3′, OH-5′, OH-4′ of myricetin to H-5 of HP-β-CD, OH-3′, OH-5′ of myricetin to H-3 of HP-β-CD, OH-3 of myricetin to H-1 and H-3 of HP-β-CD, as well as the weak correlations of H-2′ and H-6′ of myricetin to H-3 of HP-β-CD. These results indicated that the entire B ring and part of the C ring of myricetin were included in the HP-β-CD cavity (Yang, Lin, Chen, & Liu, 2009). Based on the above observations, together with the FT-IR spectrum, we deduced a possible inclusion mode for myricetin/HP-β-CD complex, as illustrated in Fig. 3C.

Recently, the inclusion modes of several flavonoid/CD complexes were investigated, and two significantly different binding modes were observed. In the present study, the myricetin/HP-β-CD inclusion complex appears similar to one of those modes, in which the aromatic B-ring of flavonols is oriented toward the primary rim of the CD. Other flavonoids, such as alpinetin (Ma et al., 2012) and naringenin (Yang et al., 2013), were also considered to form the inclusion complex with CDs by similar molecular inclusion mechanisms. Furthermore, Kim, Choi, et al. (2009) also reported the same inclusion modes of the myricetin/HP-β-CD complex by molecular modeling studies. However, in the case of HP-β-CD complexes, the opposite inclusion mode, in which the A-ring of flavonols is oriented toward the primary rim of the CD, was also found in

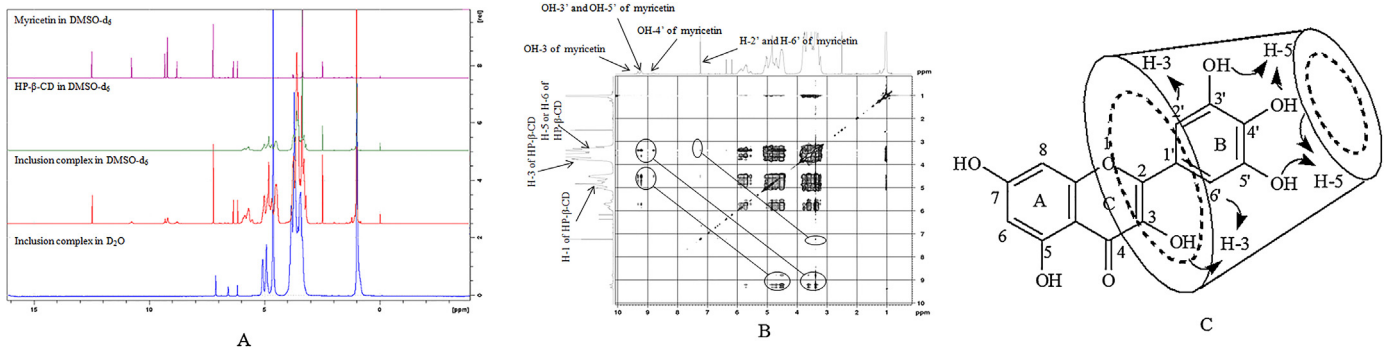

Fig. 3. ^{1}H NMR spectra of myricetin, HP-β-CD, inclusion complex in DMSO-d_6, and the inclusion complex in D_2O (A), NOESY spectrum of the myricetin/HP-β-CD complex in DMSO-d_6 (B), possible inclusion mode and significant NOESY (→) correlations of the myricetin/HP-β-CD inclusion complex (C).

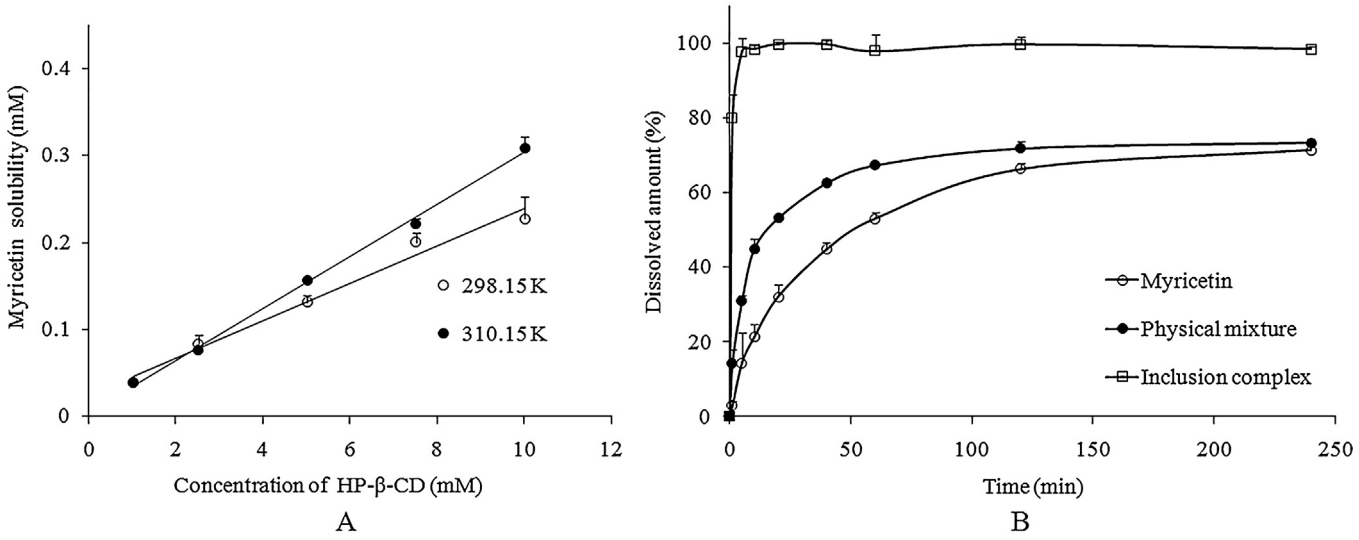

Fig. 4. Phase solubility diagram of the myricetin/HP-β-CD inclusion complex in water at 37 °C and 25 °C, respectively (A), and dissolution profiles for raw myricetin, the myricetin/HP-β-CD inclusion complex, and the physical mixture at the same ratio (B). Each data point indicates the average of three independent determinations, and the error bars indicate the standard deviation of three measurements.

Kim's research (Kim, Choi, et al., 2009). This mode was also demonstrated by the inclusion of myricetin within β-CD by molecular docking analysis (Chakraborty, Basu, & Basak, 2014). Therefore, it can be deduced that the binding mode might depend on the structural characteristics of flavonoids and the types of native/modified CDs. Specific guest molecules could most likely interact with CDs through different binding modes, and the exact mechanism should be verified by future research.

3.2. In vitro evaluations

3.2.1. Phase solubility studies

Fig. 4A shows the phase solubility diagram of myricetin in the presence of various HP-β-CD concentrations at 25 °C and 37 °C. The aqueous solubility of myricetin increased linearly ($r^2 \geq 0.98$) with increasing HP-β-CD concentration within the studied concentration range, and this linear host–guest correlation can be classified as A_L type according to Higuchi and Connors (1965). The slopes were less than 1 (i.e., 0.0214 and 0.0299 at 25 °C and 37 °C, respectively), suggesting that formation of the complexes was of the first order with respect to CD concentration (Fernandes, Vieira, & Veiga, 2002), and displayed a 1:1 stoichiometry over the concentration range (0–10 mM). Additionally, the solubility of myricetin was significantly increased (19.12-fold and 19.58-fold at 10 mM of HP-β-CD) compared to in the absence of HP-β-CD, which indicated the solubilizing potential for myricetin by HP-β-CD.

The stability constants (K_s) of myricetin/HP-β-CD were 1837.08 M^{-1} and 1956.20 M^{-1} (Table 1) at 25 °C and 37 °C, respectively. The comparatively high K_s values at each temperature suggest a favorable spatial relationship between myricetin and HP-β-CD (Wong & Yuen, 2003). Generally, the stability constant value can describe the strength or magnitude of complexation of drug within the CD cavity. Hence, the K_s of myricetin/HP-β-CD at 37 °C was larger than at 25 °C, meaning a relatively high temperature promoted formation of the complex. A similar phenomenon was also observed in Simvastatin/HP-β-CD inclusion complex studies (Jun et al., 2007), while the opposite trend, K_s decreased with the increase of temperature, was exhibited in a rutin/HP-β-CD inclusion complex (Nguyen et al., 2013). These opposing tendencies suggest that reaction temperature is a very important factor of complex formation.

The change in the thermodynamic parameters, namely Gibbs free energy, enthalpy and entropy (ΔG, ΔH, and ΔS), of the complexation reaction were calculated and are shown in Table 1. The negative ΔG values (−18.55 kJ mol^{-1} and −18.71 kJ mol^{-1} at 25 °C and 37 °C, respectively) demonstrated the spontaneity of the complexing process with HP-β-CD (Pandit et al., 2011) and suggest that HP-β-CD solutions could offer a favorable environment for myricetin. We determined a positive ΔH for complexation of myricetin with HP-β-CD, predicting it to be an endothermic process. Thus, energy was required for the displacement of water or the formation of non-covalent bonds between myricetin and HP-β-CD. Moreover, positive ΔS was indicated an increase in the randomness of this system. The possible reason was that myricetin molecules still have some conformational freedom after being complexed, and the released water molecules also resulted in an increase in the randomness of the entire system (Wong & Yuen, 2003). Jun et al. also observed the similar changes of simvastatin/HP-β-CD inclusion complex with negative ΔG, positive ΔH and ΔS (Jun et al., 2007). In brief, the complexation of myricetin and HP-β-CD took place spontaneously, and a relatively high temperature was preferred.

3.2.2. Dissolution studies

The dissolution profiles of the myricetin/HP-β-CD inclusion complex compared with myricetin powder and the physical mixture of myricetin and HP-β-CD at the same ratios are shown in Fig. 4B. Considering the extremely low solubility of myricetin, 0.1% Tween-80 was utilized as the dissolution medium. As observed from the profiles, free myricetin showed a limited dissolution of

Table 1
The stability constant (K_s), and the thermodynamic parameters of myricetin/HP-β-CD inclusion complex obtained from the phase solubility diagram.

T (K)	S_0 (mM)	Slope	K_s (M^{-1})	ΔG (kJ mol^{-1})	ΔH (kJ mol^{-1})	ΔS (J mol^{-1} K^{-1})
298.15	$11.90 \pm 1.02 \times 10^{-3}$	0.0214	1837.08	−18.55	4.01	75.67
310.15	$15.76 \pm 0.59 \times 10^{-3}$	0.0299	1956.20	−18.71	4.01	73.25

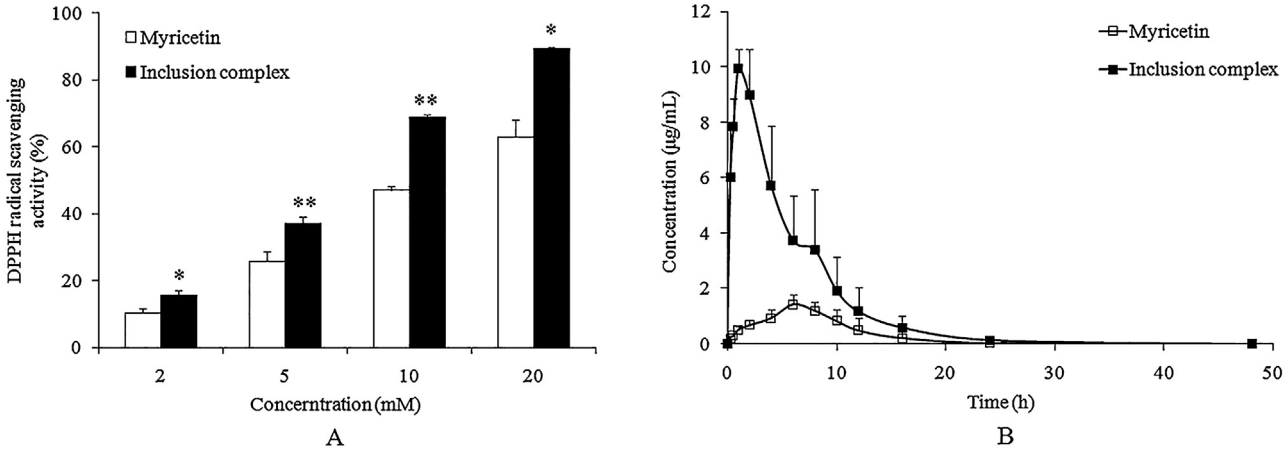

Fig. 5. Percentage inhibition of DPPH radical scavenging activity by myricetin and the myricetin/HP-β-CD inclusion complex in 0.1% Tween-80 (A). Each data point indicates the average of three independent determinations, and the error bars indicate the standard deviation of three measurements. $^{*}p < 0.05$ and $^{**}p < 0.01$ compared to free myricetin. Plasma concentration–time curves of myricetin for myricetin coarse powder at a dose of 50 mg/kg of myricetin and the myricetin/HP-β-CD inclusion complex at a dose of 25 mg/kg of myricetin after oral administration to rats ($n = 6$) (B).

less than 60% and 75% at 60 and 240 min points, respectively. In contrast, the complex exhibited much faster dissolution than the corresponding physical mixture and myricetin, with an accumulative dissolution over 98% within 10 min, and dissolved completely within 20 min. These facts were consistent with the results of the enhanced solubility of myricetin shown in phase solubility studies. Moreover, the reduction in the crystallinity of myricetin, its conversion to an amorphous form after complexing, as indicated in PXRD and SEM section (Fig. 2), and the increased wettability (Zhou, Wei, Dou, Chou, & Wang, 2013) likely contributed to the enhanced dissolution of the complex. Furthermore, the surfactant properties of CDs, which reduce the interfacial tension between drug and dissolution medium, could cause an increase in the drug dissolution rate (de Freitas et al., 2012; Soares-Sobrinho et al., 2012; Zhou et al., 2013). Thus, the presence of HP-β-CD in the physical mixture also resulted in some dissolution improvement and exhibited a dissolution amount of 66% at 60 min but was almost the same as that of pure myricetin at 240 min because no complex formed.

In short, it can be concluded that the myricetin/HP-β-CD complex exhibited much faster dissolution than the pure drug; this enhanced dissolution is expected translate to an improved oral bioavailability of the drug. The results obtained in this study confirmed again that the complexation of poorly soluble drugs with cyclodextrins can be used as an effective formulation strategy to enhance solubility and dissolution rate.

3.2.3. Assay of antioxidant activities

The results of comparisons the antioxidant effects of myricetin and myricetin/HP-β-CD inclusion complex in two solutions: 50% ethanol (data not shown) and 0.1% Tween-80 (Fig. 5A) were obtained from the DPPH radical scavenging assay. Both the scavenging activities of myricetin and its complex were concentration dependent within the evaluated range. Interestingly, no significant change was observed for myricetin in 50% ethanol after complexing with HP-β-CD. Since the antioxidant activities might mainly depend on the hydrogen-donating capacity of the pyrogallol moiety on the B ring of myricetin (Kwon, Kim, Park, & Jung, 2010). Myricetin/HP-β-CD inclusion complex consumes almost same amount of DPPH molecular with free myricetin at equivalent concentrations because the hydrogen-donating capacity of myricetin could not be changed after complexion. Additionally, CDs had no effect on the antioxidant activity, reported by Chakraborty et al. (2014), which might be another probable reason for the unchanged antioxidant effects of the myricetin/HP-β-CD inclusion complex.

As shown in Fig. 5A, an obvious enhanced scavenging effect of the complex in 0.1% Tween-80 compared to the free myricetin was observed: the scavenging rate reached 89.27% at 20 mM of the complex, with only 62.96% for myricetin. Due to the poor aqueous solubility, raw myricetin was unable to completely disperse in the solvents; subsequently, myricetin molecules could not fully interact and react with the odd electron of DPPH. Thus, increases in the antioxidant activity of the myricetin complex with HP-β-CD can likely be attributed to its enhanced solubility. Similar results for the rutin/HP-β-CD complex was reported by Nguyen et al. (2013) showing stronger antioxidant activity in comparison with free rutin, which was also likely related to the improvement in its solubility. These results also indicate that complex formation could be useful to maintain and even enhance the antioxidant activity of drugs.

3.3. In vivo pharmacokinetics

The mean plasma concentrations of myricetin versus time are given in Fig. 5B, from which it can be observed that the pharmacokinetic profile of the inclusion complex showed a clear advantage over pure myricetin. As expected, the plasma concentration of the complex was much higher than that of myricetin within 48 hours. Interestingly, a weak "shoulder-peak" was observed in the C–t curve of myricetin/HP-β-CD inclusion complex, while a single peak was detected in the curve of pure myricetin (50 mg/kg), which was similar to the change of plasma concentration profiles of artemether in rats after intragastric gavage of its pure drug and HP-β-CD complex (Yang et al., 2009). This phenomenon indicated that myricetin exhibited poor enterohepatic recirculation, such as other flavonoids (Li et al., 2012), and that it could be improved by complex formation.

The pharmacokinetic parameters of myricetin as a coarse powder and as a CD complex are listed in Table 2. The maximum levels in plasma (C_{max}) of the myricetin complex group were significantly ($p < 0.01$) enhanced 6.93-fold compared to that of the pure myricetin. The time required to reach C_{max} (T_{max}) of myricetin was statistically accelerated ($p < 0.01$) from 6.4 ± 0.89 h for the pure myricetin to 1.2 ± 0.45 h for myricetin/HP-β-CD inclusion complex. The area under the plasma concentration $AUC_{0-48\,h}$ after oral administration of myricetin/HP-β-CD inclusion complex was much higher, and the mean residence times in the plasma (MRT)

Table 2
Pharmacokinetic parameters of myricetin (50 mg/kg) and myricetin/HP-β-CD inclusion complex (25 mg/kg) after oral administration of rats (values are mean ± SD, $n = 6$).

Parameters	Formulation	
	Myricetin	Inclusion complex
C_{max} (μg/mL)	1.49 ± 0.20	10.33 ± 0.56**
T_{max} (h)	6.40 ± 0.89	1.20 ± 0.45**
$t_{1/2}$ (h)	2.78 ± 0.81	3.75 ± 0.53
AUC_{0-t} (μg h mL^{-1})	13.72 ± 5.58	64.50 ± 22.10*
$AUC_{0-\infty}$ (μg h mL^{-1})	13.73 ± 5.58	64.51 ± 22.10*
MRT (h)	7.88 ± 1.80	5.48 ± 1.32*
Relative bioavailability (%)	–	940.11

*$p < 0.05$ and **$p < 0.01$ as compared to myricetin group after oral administration (50 mg/kg), respectively.

were significantly shorter ($p < 0.05$) than those of myricetin coarse powder. Moreover, the relative bioavailability of the myricetin/HP-β-CD inclusion complex was calculated to be 940.11% that of myricetin, revealing an obvious improvement of oral absorption after complexation with HP-β-CD. Moreover, the elimination half-life ($t_{1/2}$) of the inclusion complex was prolonged from 2.78 ± 0.81 h to 3.75 ± 0.53 h, providing more time for absorption than the coarse myricetin powder.

Several factors could be involved in the improvement of the oral bioavailability of myricetin, such as membrane permeation enhancement, an increased solubility/dissolution rate, rapid metabolism or elimination prevention (Zhang et al., 2013). In the present investigation, the enhanced solubility and dissolution rate were apparently the prominent reason for the higher C_{max} and AUC of myricetin obtained after oral administration of the myricetin/HP-β-CD inclusion complex. Moreover, the prolonged $t_{1/2}$ of inclusion complex might reduce the clearance rate and provide sufficient time for absorption of myricetin because its stability in intestinal fluid might be enhanced after complexing (Zheng, Haworth, Zuo, Chow, & Chow, 2005; Kurkov & Loftsson, 2013; Yao et al., 2014). However, further investigations concerning the effects of the complex on the metabolism and excretion of myricetin were not conducted and should be undertaken in the future.

These data provided strong evidence that the oral absorption of myricetin is highly limited by its dissolution and solubility, proving that myricetin could be defined as BCS class II drugs. For these drug candidates, solubility enhancement was the principal difficulty and complexes with CDs provide a promising vehicle for their oral delivery with optimized absorption.

4. Conclusions

In this paper, a myricetin/HP-β-CD inclusion complex with a 1:1 stoichiometric ratio was successfully prepared. Myricetin was transformed from crystalline to amorphous form after complexation with HP-β-CD, as characterized by DSC, PXRD, and SEM. The molecular inclusion mechanisms determined by FT-IR and ^{1}H NMR showed that the B-ring and part of the C-ring of myricetin were encapsulated into the cavity of HP-β-CD through non-covalent bonds. The aqueous solubility and dissolution rate of myricetin/HP-β-CD inclusion complex were increased significantly compared to pure myricetin. Correspondingly, the oral bioavailability of myricetin in the myricetin/HP-β-CD inclusion complex in rats and its antioxidant activities were greatly improved. Briefly, this research applies an effective approach of complexation with CDs to overcome the limited absorption of myricetin, a poorly soluble compound in herbal medicine.

Conflict of interest

The authors report no conflicts of interest.

Acknowledgements

This study was sponsored by the Nano-Specific Project of Shanghai Science and Technology Commission (12nm0502400), the Shanghai Rising-Star Program (12QB1405100), the Innovation Program of Shanghai Municipal Education Commission (14YZ057), the Specialized Research Fund for the Doctoral Program of Higher Education (20133107120006) and the First-class Subjects of Chinese Materia Medica (ZYX-NSFC-013). The authors are grateful to Professor Guixin Chou for the analytical guidance of the NMR data.

References

Adibkia, K., Barzegar-Jalali, M., Maheri-Esfanjani, H., Ghanbarzadeh, S., Shokri, J., Sabzevari, A., et al. (2013). Physicochemical characterization of naproxen solid dispersions prepared via spray drying technology. *Powder Technology*, *246*, 448–455.

Burton, L., Ying, W., Gandhi, R., West, R., Huang, C., Zhou, S., et al. (2012). Development of a precipitation-resistant solution formulation to increase in vivo exposure of a poorly water-soluble compound. *International Journal of Pharmaceutics*, *433*, 94–101.

Chakraborty, S., Basu, S., & Basak, S. (2014). Effect of β-cyclodextrin on the molecular properties of myricetin upon nano-encapsulation: Insight from optical spectroscopy and quantum chemical studies. *Carbohydrate Polymers*, *99*, 116–125.

Dajas, F., Rivera, F., Blasina, F., Arredondo, F., Echeverry, C., Lafon, L., et al. (2003). Cell culture protection and in vivo neuroprotective capacity of flavonoids. *Neurotoxicity Research*, *5*, 425–432.

Dang, Y., Lin, G., Xie, Y., Duan, J., Ma, P., Li, G., et al. (2013). Quantitative determination of myricetin in rat plasma by ultra performance liquid chromatography tandem mass spectrometry and its absolute bioavailability. *Drug Research*, http://dx.doi.org/10.1055/s-0033-1363220

de Freitas, M. R., Rolim, L. A., Soares, M. F. D., Rolim-Neto, P. J., de Albuquerque, M. M., & Soares-Sobrinho, J. L. (2012). Inclusion complex of methyl-beta-cyclodextrin and olanzapine as potential drug delivery system for schizophrenia. *Carbohydrate Polymers*, *89*, 1095–1100.

Delrivo, A., Zoppi, A., & Longhi, M. R. (2012). Interaction of sulfadiazine with cyclodextrins in aqueous solution and solid state. *Carbohydrate Polymers*, *87*, 1980–1988.

Fernandes, C. M., Vieira, M. T., & Veiga, F. J. (2002). Physicochemical characterization and in vitro dissolution behavior of nicardipine–cyclodextrins inclusion compounds. *European Journal of Pharmaceutical Sciences*, *15*, 79–88.

Ge, X., Huang, Z., Tian, S., Huang, Y., & Zeng, C. (2012). Complexation of carbendazim with hydroxypropyl-beta-cyclodextrin to improve solubility and fungicidal activity. *Carbohydrate Polymers*, *89*, 208–212.

Gould, S., & Scott, R. C. (2005). 2-Hydroxypropyl-beta-cyclodextrin (HP-beta-CD): A toxicology review. *Food and Chemical Toxicology*, *43*, 1451–1459.

Han, M., Yu, X., Guo, Y., Wang, Y., Kuang, H., & Wang, X. (2014). Honokiol Nanosuspensions: Preparation, increased oral bioavailability and dramatically enhanced biodistribution in the cardio-cerebro-vascular system. *Colloids and Surfaces B: Biointerfaces*, http://dx.doi.org/10.1016/j.colsurfb.2013.12.056

Higuchi, T., & Connors, K. A. (1965). Phase-solubility techniques. *Advances in Analytical Chemistry Instrumentation*, *4*, 117–212.

Jullian, C., Moyano, L., Yañez, C., & Olea-Azar, C. (2007). Complexation of quercetin with three kinds of cyclodextrins: An antioxidant study. *Spectrochimica acta. Part A, Molecular and Biomolecular Spectroscopy*, *67*, 230–234.

Jun, S. W., Kim, M. S., Kim, J. S., Park, H. J., Lee, S., Woo, J. S., et al. (2007). Preparation and characterization of simvastatin/hydroxypropyl-beta-cyclodextrin inclusion complex using supercritical antisolvent (SAS) process. *European Journal of Pharmaceutics and Biopharmaceutics*, *66*, 413–421.

Kakran, M., Sahoo, N. G., & Li, L. (2011). Dissolution enhancement of quercetin through nanofabrication, complexation, and solid dispersion. *Colloids and Surfaces B: Biointerfaces*, *88*, 121–130.

Kane, R., Naik, S., Bumrela, S., & Kuchekar, B. (2009). Preparation, physicochemical characterization, dissolution and formulation studies of irbesartan cyclodextrin inclusion complexes: Comparison between β-CD & HP-β-CD. *Journal of Pharmacy Research*, *2*, 1359–1364.

Kim, H. Y., Choi, J. W., & Jung, S. (2009). Inclusion complexes of modified cyclodextrins with some flavonols. *Journal of Inclusion Phenomena and Macrocyclic Chemistry*, *64*, 43–47.

Kim, M. K., Park, K. S., Yeo, W. S., Choo, H., & Chong, Y. (2009). In vitro solubility, stability and permeability of novel quercetin–amino acid conjugates. *Bioorganic & Medicinal Chemistry*, *17*, 1164–1171.

Ko, C. H., Shen, S. C., Lee, T. J., & Chen, Y. C. (2005). Myricetin inhibits matrix metalloproteinase 2 protein expression and enzyme activity in colorectal carcinoma cells. *Molecular Cancer Therapeutics*, *4*, 281–290.

Kurkov, S. V., & Loftsson, T. (2013). Cyclodextrins. *International Journal of Pharmaceutics*, *453*, 167–180.

Kwon, Y. E., Kim, H. M., Park, S. Y., & Jung, S. H. (2010). Enhancement of solubility and antioxidant activity of some flavonoids based on the inclusion complexation with sulfobutylether β-cyclodextrin. *Bulletin of the Korean Chemical Society*, *31*, 3035–3037.

Li, G., Zeng, X., Xie, Y., Cai, Z., Moore, J. C., Yuan, X., et al. (2012). Pharmacokinetic properties of isorhamnetin, kaempferol and quercetin after oral gavage of total flavones of *Hippophae rhamnoides* L. in rats using a UPLC-MS method. *Fitoterapia*, *83*, 182–191.

Li, Y., & Ding, Y. (2012). Minireview: Therapeutic potential of myricetin in diabetes mellitus. *Food Science and Human Wellness*, *1*, 19–25.

Liu, I. M., Tzeng, T. F., Liou, S. S., & Lan, T. W. (2007). Myricetin, a naturally occurring flavonol, ameliorates insulin resistance induced by a high-fructose diet in rats. *Life Sciences*, *81*, 1479–1488.

Lu, L., Qian, D., Guo, J., Qian, Y., Xu, B., Sha, M., et al. (2013). Abelmoschi Corolla non-flavonoid components altered the pharmacokinetic profile of its flavonoids in rat. *Journal of Ethnopharmacology*, *148*, 804–811.

Lucas-Abellán, C., Mercader-Ros, M. T., Zafrilla, M. P., Gabaldón, J. A., & Núñez-Delicado, E. (2011). Comparative study of different methods to measure antioxidant activity of resveratrol in the presence of cyclodextrins. *Food and Chemical Toxicology*, *49*, 1255–1260.

Ma, S. X., Chen, W., Yang, X. D., Zhang, N., Wang, S. J., Liu, L., et al. (2012). Alpinetin/hydroxypropyl-beta-cyclodextrin host–guest system: Preparation, characterization, inclusion mode, solubilization and stability. *Journal of Pharmaceutical and Biomedical Analysis*, *67-68*, 193–200.

Maheshwari, D. T., Yogendra Kumar, M. S., Verma, S. K., Singh, V. K., & Singh, S. N. (2011). Antioxidant and hepatoprotective activities of phenolic rich fraction of Seabuckthorn (*Hippophae rhamnoides* L.) leaves. *Food and Chemical Toxicology*, *49*, 2422–2428.

Miyake, K., Arima, H., Hirayama, F., Yamamoto, M., Horikawa, T., Sumiyoshi, H., et al. (2000). Improvement of solubility and oral bioavailability of rutin by complexation with 2-hydroxypropyl-β-cyclodextrin. *Pharmaceutical Development and Technology*, *5*, 399–407.

Nguyen, T. A., Liu, B. G., Zhao, J., Thomas, D. S., & Hook, J. M. (2013). An investigation into the supramolecular structure, solubility, stability and antioxidant activity of rutin/cyclodextrin inclusion complex. *Food Chemistry*, *136*, 186–192.

Ong, K. C., & Khoo, H. E. (1997). Biological effects of myricetin. *General Pharmacology*, *29*, 121–126.

Ouyang, H. Z., Fang, L., Zhu, L., Zhang, L., Ren, X. L., He, J., et al. (2011). Effect of external factors on the curcumin/2-hydroxypropyl-β-cyclodextrin: In vitro and in vivo study. *Journal of Inclusion Phenomena and Macrocyclic Chemistry*, *73*, 423–433.

Pandit, V., Gorantla, R., Devi, K., Pai, R. S., & Sarasija, S. (2011). Preparation and characterization of pioglitazone cyclodextrin inclusion complexes. *Journal of Young Pharmacists*, *3*, 267–274.

Phillips, P. A., Sangwan, V., Borja-Cacho, D., Dudeja, V., Vickers, S. M., & Saluja, A. K. (2011). Myricetin induces pancreatic cancer cell death via the induction of apoptosis and inhibition of the phosphatidylinositol 3-kinase (PI3K) signaling pathway. *Cancer Letters*, *308*, 181–188.

Reddy, M. N., Rehana, T., Ramakrishna, S., Chowdhary, K. P., & Diwan, P. V. (2004). Beta-cyclodextrin complexes of celecoxib: Molecular-modeling, characterization, and dissolution studies. *AAPS PharmSciTech*, *6*, E7.

Sahoo, N. G., Kakran, M., Shaal, L. A., Li, L., Muller, R. H., Pal, M., et al. (2011). Preparation and characterization of quercetin nanocrystals. *Journal of Pharmaceutical Sciences*, *100*, 2379–2390.

Sigfridsson, K., Lundqvist, A. J., & Strimfors, M. (2009). Particle size reduction for improvement of oral absorption of the poorly soluble drug UG558 in rats during early development. *Drug Development and Industrial Pharmacy*, *35*, 1479–1486.

Soares-Sobrinho, J. L., Santos, F. L. A., Lyra, M. A. M., Alves, L. D. S., Rolim, L. A., Lima, A. A. N., et al. (2012). Benznidazole drug delivery by binary and multicomponent inclusion complexes using cyclodextrins and polymers. *Carbohydrate Polymers*, *89*, 323–330.

Stegemann, S., Leveiller, F., Franchi, D., de Jong, H., & Linden, H. (2007). When poor solubility becomes an issue: From early stage to proof of concept. *European Journal of Pharmaceutical Sciences*, *31*, 249–261.

Villaño, D., Fernández-Pachón, M. S., Moyá, M. L., Troncoso, A. M., & García-Parrilla, M. C. (2007). Radical scavenging ability of polyphenolic compounds towards DPPH free radical. *Talanta*, *71*, 230–235.

Wong, J. W., & Yuen, K. H. (2003). Inclusion complexation of artemisinin with alpha-, beta-, and gamma-cyclodextrins. *Drug Development and Industrial Pharmacy*, *29*, 1035–1044.

Yang, B., Lin, J., Chen, Y., & Liu, Y. (2009). Artemether/hydroxypropyl-beta-cyclodextrin host–guest system: Characterization, phase-solubility and inclusion mode. *Bioorganic & Medicinal Chemistry*, *17*, 6311–6317.

Yang, L. J., Ma, S. X., Zhou, S. Y., Chen, W., Yuan, M. W., Yin, Y. Q., et al. (2013). Preparation and characterization of inclusion complexes of naringenin with beta-cyclodextrin or its derivative. *Carbohydrate Polymers*, *98*, 861–869.

Yao, Y., Lin, G., Xie, Y., Ma, P., Li, G., Meng, Q., et al. (2014). Preformulation studies of myricetin: A natural antioxidant flavonoid. *Die Pharmazie*, *69*, 19–26.

Yuan, C., Du, L., Jin, Z. Y., & Xu, X. M. (2013). Storage stability and antioxidant activity of complex of astaxanthin with hydroxypropyl-beta-cyclodextrin. *Carbohydrate Polymers*, *91*, 385–389.

Yuan, C., Jin, Z. Y., & Xu, X. (2012). Inclusion complex of astaxanthin with hydroxypropyl-beta-cyclodextrin: UV, FTIR, H-1 NMR and molecular modeling studies. *Carbohydrate Polymers*, *89*, 492–496.

Zhang, J. J., Huang, Y. T., Liu, D. P., Gao, Y., & Qian, S. (2013). Preparation of apigenin nanocrystals using supercritical antisolvent process for dissolution and bioavailability enhancement. *European Journal of Pharmaceutical Sciences*, *48*, 740–747.

Zheng, Y., Haworth, I. S., Zuo, Z., Chow, M. S., & Chow, A. H. (2005). Physicochemical and structural characterization of quercetin–beta-cyclodextrin complexes. *Journal of Pharmaceutical Sciences*, *94*, 1079–1089.

Zhou, Q. N., Wei, X. H., Dou, W., Chou, G. X., & Wang, Z. T. (2013). Preparation and characterization of inclusion complexes formed between baicalein and cyclodextrins. *Carbohydrate Polymers*, *95*, 733–739.